Seizure Prediction by Graph Mining and Transfer Learning

Anonymous Author(s)
Affiliation
Address
email

Abstract

Abstract goes here.

1 Introduction

Epilepsy is one of the most common disorders of the central nervous system characterized by recurring seizures. An epileptic seizure is described by abnormally excessive or synchronous neuronal activity in the brain [4]. Epilepsy patients show no pathological signs of the disease during inter-seizure periods, however, the uncertainty with regards to the onset of the next seizure deeply affects the lives of the patients [5].

In [14] the authors posed the question whether characteristic features can be extracted from the continuous EEG signal that are predictive of an impending seizure. If it were possible to reliably predict seizure occurrence then preventive clinical strategies would be replaced by patient specific proactive therapy such as reseting brain by electrical or other stimulation. While clinical studies show early indicators for a pre-seizure state including increased cerebral blood flow, heart rate change, the research in seizure prediction is still not reliable for clinical use.

In general approaches to seizure prediction problem share several common steps including processing of multichannel EEG signals (i) discretize the time series into sliding windows with a constant number and overlapping epochs (ii) to extract sub-frequencies, to analyze the signal in frequency and/or time domain using (e.g., using wavelength transformation [1]), (iii) extract features either directly from the signal or from transformations. These featues can be univariate computed on each EEG channel separately or bivariate computed between two or more EEG channels they can be linear or nonlinear (e.g., [15]. A list of features used in characterization of epileptic seizure dynamics can be found in recent studies [15,16,22].

A particular bivariate EEG feature, which captures brainwave synchronization patterns, is shown to be an important one to differentiate interictal, preictal and ictal states [8,9]. In particular, it is suggested that interictal period is characterized by moderate synchronization at large frequency bands while preictal period is marked by a decrease in the beta range synchronization between the epileptic focus and other brain areas, followed by a subsequent hypersynchronization at the seizure onset [13].

Recently there has been increasing focus in analyzing EEG recordings by building a *synchronization graph* that enable characterization of the pairwise correlations between electrodes using graph theoretical features over time [2,19]. In the spatio-temporal EEG graphs, *nodes* (vertices) represent the EEG channels and the *edges* (links) represent the level of neuronal synchronization between the different regions of the brain. This approach has been exploited in the analysis of various neuropsychiatric diseases including schizophrenia and autism, dementia, and epilepsy [19]. Within epilepsy research, evolution of certain graph features over time revealed better understanding of the interactions of the brain regions and the seizures. For instance, Schindler et. al. analyzed the change in path

lengths and clustering coefficients to highlight the evolution of seizures on epileptic patients [17], Kramer et. al. considered the evolution of local graph features including betweenness centrality to explain the coupling of brain signals at seizure onset [7], and Douw et. al. recently showed epilepsy in glioma patients was attributed to the theta band activity in the brain [3]. In [12] authors independently suggest a similar approach that combines tensor decompositions with graph theory. In this paper, we continue studying synchronization graphs and introduce new features as the early indicators of a seizure onset.

The organization of the paper is as follows: in Section 2, we describe the epileptic EEG dataset 2.1, methodology to construct EEG synchronization graphs 2.3, and the computation of global and local features on these graphs 2.4. In Section 2.7, we describe the seizure prediction method. in Section 3 we present results for seizure prediction. Finally, we provide an overview, discuss the results, and list extensions to this study, in Section 4.

2 Methodology

2.1 Epileptic EEG Data Set

Our dataset consists of scalp EEG recordings of 26 seizures from 11 patients. All the patients were evaluated with scalp video-EEG monitoring in the international 10-20 system (as described in [6]), magnetic resonance imaging (MRI), fMRI for language localization, and position emission tomography (PET). All the patients had *Hippocampal Sclerosis* (HS) except one patient (IY) with *Cortical Dysplasia* (CD). After selective amygdalohippocampectomy, all the patients were seizure free. The patient information is provided in Table 1. For 4 patients, the seizure would onset from the left, whereas for 7 patients the seizure would onset from the right.

One patient has one 30 minute recording, two patients have two 30 min recordings, one patient has three 30 min recordings, one patient has single 60 minute recording, three patients have two 60 minute recordings, two patients have three 60 minute recordings, and one patient has five 60 minute recordings. The recordings include sufficient pre-ictal and post-ictal periods for the analysis. Two of the electrodes (A_1 and A_2) were unused and C_z electrode was used for referential montage that yielded 18-channel EEG recordings. A team of doctors diagnosed the initiation and the termination of each seizure and reported these periods as the ground truth for our analysis. An example of such a recording can be found in Fig.2 in [18]. Seizures were 73.81 seconds long on average and their standard deviation was 52.42 seconds.

Table 1: Patient Types. Almost all the patients (except one patient) exhibited hippocampal sclerosis (HS). There are two types of lateralizations in HS: left (L) and right (R). One patient (IY) exhibited cortical dysplasia (CD).

Patient	Pathology	Lateralization
IY	CD	R
OB	HS	R
BMI	HS	R
FZE	HS	R
GSE	HS	L
IP	HS	L
MSO	HS	L
ABA	HS	L
DAK	HS	L
NT	HS	L
SUL	HS	L

2.2 Initial Data Processing – Low Rank Approximation

2.3 Construction of EEG Synchronization Graphs

Let $\mathbf{X}[i, m]$ denote the recorded EEG signal, where $i \in \{1, \ldots, 18\}$ represents the index for the ith electrode and $m \in [1, \ldots, f_s \times M]$ represents the time index, f_s represents the sampling frequency, and M is the duration of the recording in seconds. Sampling frequency, f_s, is either 200 Hz or 400 Hz. We constructed epochs of equal lengths with 20% overlap between the preceding and following epochs. The number of epochs N is equal to $1.25M/L$, where L is the duration of the epoch in same time units.

Given the nature of these spatio-temporal recordings, we consider constructing *time-evolving EEG Synchronization Graphs* on the EEG datasets. A graph is constructed for each epoch. The *nodes* represent the EEG electrodes and the *edges* represent a closeness relationship between the nodes in a given epoch. The main goal sought in the time-evolving EEG synchronization graphs is the ability to sense both the spatial and temporal changes in the network, yielding measures of change for the mining.

The selection of epoch length is significant in both the time-domain and frequency-domain analysis techniques. While longer epochs provide better frequency resolution, too lengthy epochs may not be stationary [21] and not allow rapid detections of changes in the network [10,11]. Therefore, shorter epoch lengths are generally preferred. However, too short epoch lengths may not allow the generation of meaningful graphs for mining. We use an epoch length of 5 seconds. Note that if a wavelet-domain-based measure is employed for the construction of the time-evolving graphs, these effects are reduced or eliminated. However, as the range of explored frequencies must be arbitrarily defined prior to the wavelet analysis, wavelet domain techniques do not allow the simultaneous exploration of the whole range of the EEG frequency spectrum.

For purposes of illustration, we construct simple time-evolving graphs on the EEG recording shown in Fig. 1. The graph edges are established based on the pair-wise relationships between the epoch data. Specifically, an edge between two distinct nodes i and k, where $i, k \in \{1, \ldots, 18\}$, and $i \neq k$, is established if the pair-wise distance for the nth epoch, $d^n_{i,k}$, is less than the threshold τ. A parametric search is performed to find optimal values for the threshold τ. Further information about the search performed on various parameters to determine optimal values is provided in Section 3.

Several synchronization measures have been proposed as plausible options for $d^n_{i,k}$. Based on earlier results (under review), we chose Phase Lag Index [20]. PLI is defined as follows:

$$PLI_{i,k}(n) \quad = \quad \frac{1}{Lf_s} \left| \sum_{m=1}^{Lf_s} \text{sgn}\left(\phi^n_i(m) - \phi^n_k(m)\right) \right| \tag{1}$$

where $\phi^n_i = \arctan(\frac{\hat{\mathbf{x}}^n_i}{\mathbf{x}^n_i})$ is the angle of the Hilbert transform $\hat{\mathbf{x}}^n_i$ of the signal $\mathbf{x}^n_i$. Note that smaller threshold values seek higher correlation between the electrodes, therefore yield sparser graphs. Similarly, higher threshold values would establish an edge even if there is small correlation between the data, therefore would yield denser graphs.

2.4 Feature Extraction from EEG Synchronization Graphs

We extract 26 features from the EEG graph for each epoch. These features quantify the compactness, clusteredness, and uniformity of the graph. Apart from these graph-based features, we compute two spectral features - the variance of the eigenvector of the product of the adjacency matrix and the inverse of the degree matrix, and the second largest eigenvalue of the Laplacian matrix.

We also extracted *********NIVAS PLACE-HOLDER FOR CHANGE-POINT DETECTION FEATURES, REFER TABLE FOR DESCRIPTION OF FEATURES**

Compactness of a graph is measured by features such as *average eccentricity*, *diameter*, *radius*, and *number of central points* that are based on the path distances between the nodes within the graph. The *clusteredness* of a graph is measured by features such as *average clustering coefficient* and *number of connected components* that are based on how connected the nodes and their neighbors with respect to each other. In addition, we also extract *spectral graph features* such as *spectral radius* and

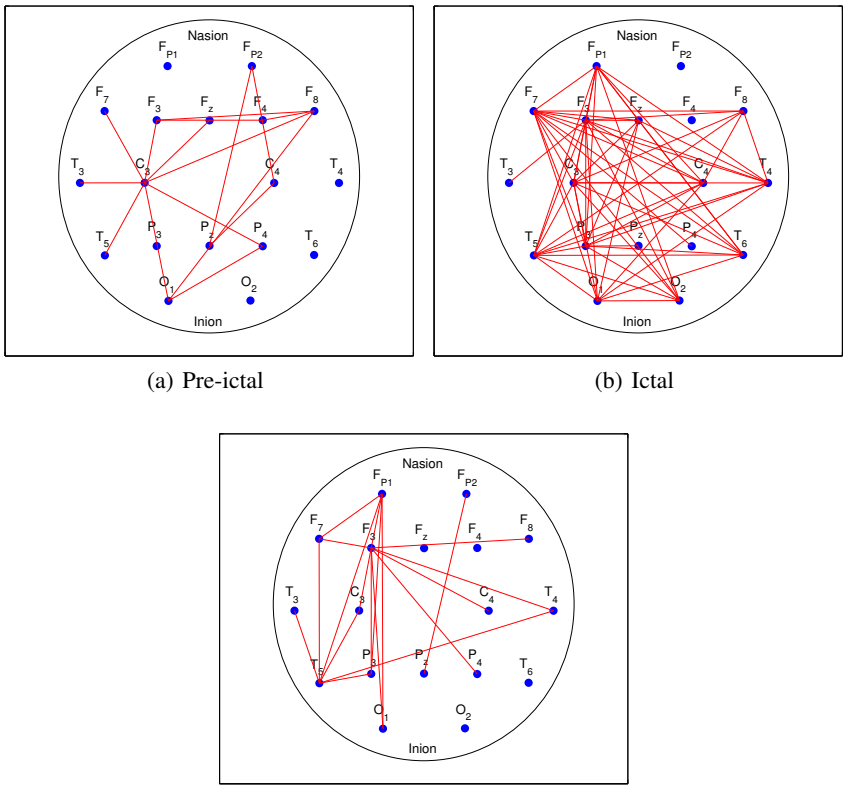

(a) Pre-ictal (b) Ictal

(c) Post-Ictal

Figure 1: **Sample EEG Synchronization Graphs for pre-ictal, ictal, and post-ictal epochs.** It is clearly seen that the ictal period has more coherence between different regions of the brain.

spectral gap using the eigenvalues of the adjacency, Laplacian, and normalized Laplacian matrices that reveal additional clusteredness and compactness properties about the graphs. A complete list of the features used in this work and their definitions is listed in Table 2.

2.5 Quadratic Programming Feature Selection

********* NIVAS PLACE-HOLDER FOR QPFS**

2.6 Transfer Learning on Features Extracted from EEG Synchronization Graphs and EEG signal

2.7 Seizure Prediction by Learning Normal Signal and Identifying Seizure as an Anomaly

********NIVAS PLACE-HOLDER FOR LEARNING ON REGULAR SIGNAL**

Table 2: Description of EEG global graph features.

Index	Feature Name	Description
1	Average Degree	Average number of edges per node
2	Clustering Coefficient C	Average of the ratio of the links a node's neighbors have in between to the total number that can possibly exist
3	Clustering Coefficient D	Same as feature 2 with node added to both numerator and denominator
4	Average Eccentricity	Average of node eccentricities, where the *eccentricity* of a node is the maximum distance from it to any other node in the graph
5	Diameter of graph	Maximum of node eccentricities
6	Radius of graph	Minimum of node eccentricities
7	Average Path Length	Average hops along the shortest paths for all possible pairs of nodes
8	Giant Connected Component Ratio	Ratio between the number of nodes in the largest connected component in the graph and total the number of nodes
9	Number of Connected Components	Number of clusters in the graph excluding the isolated nodes
10	Average Connected Component Size	Average number of nodes per connected component
11	% of Isolated Points	% of isolated nodes in the graph, where an *isolated node* has a degree 0
12	% of End Points	% of endpoints in the graph, where an *endpoint* has a degree 1
13	% of Central Points	% of nodes in the graph whose eccentricity is equal to the graph radius
14	Number of Edges	Number of edges between all nodes in the graph
15	Spectral Radius	Largest eigenvalue of the adjacency matrix
16	Adjacency Second Largest Eigenvalue	Second largest eigenvalue of the adjacency matrix
17	Adjacency Trace	Sum of the adjacency matrix eigenvalues
18	Adjacency Energy	Sum of the square of adjacency matrix eigenvalues
19	Spectral Gap	Difference between the magnitudes of the two largest eigenvalues
20	Laplacian Trace	Sum of the Laplacian matrix eigenvalues
21	Laplacian Energy	Sum of the square of Laplacian matrix eigenvalues
22	Normalized Laplacian Number of 0's	Number of eigenvalues of the normalized Laplacian matrix that are 0
23	Normalized Laplacian Number of 1's	Number of eigenvalues of the normalized Laplacian matrix that are 1
24	Normalized Laplacian Number of 2's	Number of eigenvalues of the normalized Laplacian matrix that are 2
25	Normalized Laplacian Upper Slope	The sorted slope of the line for the eigenvalues that are between 1 and 2
26	Normalized Laplacian Trace	Sum of the normalized Laplacian matrix eigenvalues
27	Mean of EEG recording	Mean of EEG signal for each electrode and epoch
28	Variance of EEG recording	Variance of EEG signal for each electrode and epoch
29,30	Change-based Features	Mean and variance of change in EEG signal for each electrode and epoch
31	Change-based Feature 3	Variance of EEG signal for particular electrode in given epoch after subtracting the mean of up to 3 previous windows
32	Spectral Feature 1	Variance of eigenvector of the product of the adjacency matrix and the inverse of the degree matrix
33	Spectral Feature 2	Second largest eigenvalue of the Laplacian matrix

3 Results

3.1 Seizure Prediction

4 Discussion and Conclusions

References

[1] E. Acar, C. A. Bingol, B. H., and Y. B. Computational analysis of epileptic focus localization. In *Fourth IASTED Int. Conf. on Biomedical Engineering*, pages 317–322, 2006.

[2] E. Bullmore and O. Sporns. Complex brain networks: graph theoretical analysis of structural and functional systems. *Nature Reviews Neuroscience*, 10(3):186–198, 2009.

[3] L. Douw, E. van Dellen, M. de Groot, J. J. Heimans, M. Klein, C. J. Stam, and J. C. Reijneveld. Epilepsy is related to theta band brain connectivity and network topology in brain tumor patients. *BMC Neuroscience*, 11(1):103, 2010.

[4] R. S. Fisher, W. van Emde Boas, W. Blume, C. Elger, P. Genton, P. Lee, and J. J. Engel. Epileptic seizures and epilepsy: definitions proposed by the international league against epilepsy (ilae) and the international bureau for epilepsy (ibe). *Epilepsia*, 46(4):470–472, 2005.

[5] R. S. Fisher, B. G. Vickrey, P. Gibson, B. Hermann, P. Penovich, A. Scherer, and S. Walker. The impact of epilepsy from the patient's perspective I. descriptions and subjective perceptions. *Epilepsy Research*, 41(1):39–51, 2000.

[6] H. H. Jasper. The ten-twenty electrode system of the international federation. *Electroencephalogr Clin Neurophysiol Suppl.*, 10:371–375, 1958.

[7] M. A. Kramer, E. D. Kolaczyk, and H. E. Kirsch. Emergent network topology at seizure onset in humans. *Epilepsy Research*, 79(2):173–186, 2008.

[8] Q. M. Le Van, V. Navarro, J. Martinerie, M. Baulac, and V. F. J. Toward a neurodynamical understanding of ictogenesis. *Epilepsia*, 44(12):30–43, 2003.

[9] Q. M. Le Van, J. Soss, V. Navarro, R. Robertson, M. Chavez, M. Baulac, and J. Martinerie. Preictal state identification by synchronization changes in long-term intracranial EEG recordings. *Clinical Neurophysiology*, 116:559–568, 2005.

[10] W. J. Levy. The effect of epoch length on the identification of changes in EEG power spectra. *Anesthesiology*, 65(3A):A539, 1986.

[11] W. J. Levy. The effect of epoch length on the identification of changes in EEG power spectra. *Anesthesiology*, 66(4):489–495, 1987.

[12] A. Mahyari and S. Aviyente. Identification of dynamic functional brain network states through tensor decomposition. In *39th IEEE International Conference on Acoustics, Speech, and Signal Processing (ICASSP 2014)*, 2014.

[13] P. Mirowski, D. Madhavan, Y. LeCun, and R. Kuzniecky. Classification of patterns of EEG synchronization for seizure prediction. *Clinical Neurophysiology*, 120:1927–1940, 2009.

[14] F. Mormann, R. G. Andrzejak, C. E. Elger, and K. Lehnertz. Seizure prediction: the long and winding road. *Brain*, 130:314–333, 2007.

[15] F. Mormann, T. Kreuz, C. Rieke, R. Andrzejak, A. Kraskov, P. David, C. Elger, and K. Lehnertz. On the predictability of epileptic seizures. *Clinical neurophysiology*, 116(3):569–587, 2005.

[16] N. Päivinen, S. Lammi, A. Pitkänen, J. Nissinen, M. Penttonen, and T. Grönfors. Epileptic seizure detection: A nonlinear viewpoint. *Computer methods and programs in biomedicine*, 79(2):151–159, 2005.

[17] K. A. Schindler, S. Bialonski, M.-T. Horstmann, C. E. Elger, and K. Lehnertz. Evolving functional network properties and synchronizability during human epileptic seizures. *CHAOS: An Interdisciplinary Journal of Nonlinear Science*, 18(3):033119, 2008.

[18] S. J. M. Smith. EEG in the diagnosis, classification, and management of patients with epilepsy. *J Neurol Neurosurg Psychiatry*, 76:ii2–i–i7, 2005.

[19] C. Stam and E. van Straaten. The organization of physiological brain networks. *Clinical Neurophysiology*, 2012.

[20] C. J. Stam, G. Nolte, and A. Daffertshofer. Phase lag index: Assessment of functional connectivity from multi channel EEG and MEG with diminished bias from common sources. *Human Brain Mapping*, 28:1178–1193, 2007.

[21] M. van de Velde, I. R. Ghosh, and P. J. M. Cluitmans. Context related artefact detection in prolonged EEG recordings. *Computer Methods and Programs in Biomedicine*, 60(3):183–196, 1999.

[22] M. J. A. M. van Putten, T. Kind, F. Visser, and V. Lagerburg. Detecting temporal lobe seizures from scalp EEG recordings: a comparison of various features. *Clinical neurophysiology*, 116(10):2480–2489, 2005.